DOI: 10.1002/chem.200500214

Studies of "Pinwheel-Like" Bis[1,8,15,22-tetrakis(3-pentyloxy)-phthalocyaninato] Rare Earth(III) Double-Decker Complexes

Rongming Wang,[a] Renjie Li,[a] Yongzhong Bian,[a] Chi-Fung Choi,[b] Dennis K. P. Ng,*[b] Jianmin Dou,[c] Daqi Wang,[c] Peihua Zhu,[a] Changqin Ma,[a] Regan D. Hartnell,[d] Dennis P. Arnold,[d] and Jianzhuang Jiang*[a]

Abstract: Homoleptic bis(phthalocyaninato) rare-earth double-deckers complexes $[M^{III}\{Pc(\alpha\text{-}OC_5H_{11})_4\}_2]$ (M = Eu, Y, Lu; $Pc(\alpha\text{-}OC_5H_{11})_4$ = 1,8,15,22-tetrakis(3-pentyloxy)phthalocyaninate) have been prepared by treating the metal-free phthalocyanine $H_2Pc(\alpha\text{-}OC_5H_{11})_4$ with the corresponding $M(acac)_3{\cdot}nH_2O$ (acac = acetylacetonate) in refluxing *n*-octanol. Due to the C_{4h} symmetry of the $Pc(\alpha\text{-}OC_5H_{11})_4$ ligand and the double-decker structure, all the reactions give a mixture of two stereoisomers with C_{4h} and D_4 symmetry. The former isomer, which is a major product, can be partially separated by recrystallization due to its higher crystallinity. The molecular structure of the major isomer of the Y analogue has been determined by single-crystal X-ray diffraction analysis. The metal center is eight-coordinate bound to the isoindole nitrogen atoms of the two phthalocyaninato ligands, forming a distorted square antiprism. Such an arrangement leads to an interesting "pinwheel" structure when viewed along the C_4 axis, which assumes a very unusual S_8 symmetry. The major isomers of all these double-deckers have also been characterized with a wide range of spectroscopic methods. A systematic investigation of their electronic absorption and electrochemical data reveals that the π–π interaction between the two $Pc(\alpha\text{-}OC_5H_{11})_4$ rings is weaker than that for the corresponding unsubstituted or β-substituted bis(phthalocyaninato) analogues.

Keywords: lanthanides · phthalocyanines · sandwich complexes · structure elucidation · yttrium

Introduction

Bis(phthalocyaninato) rare-earth complexes have been intensively studied as an important and useful class of advanced materials for gas sensors, electrochromic displays, photoconductors, other opto-electronic devices, and single-molecular magnets.[1–4] To date, most of the studies have focused on double-deckers with either unsubstituted phthalocyaninato ligands or the tetra- or octa-β-substituted analogues (i.e., substituted at the 2, 3, 9, 10, 16, 17, 23, and 24 positions).[5] Sandwich-type complexes with α-substituted phthalocyaninato ligands are extremely rare.[6] Due to the very different electronic properties of α-substituted phthalocyanines and the β-substituted counterparts,[7] we were interested to examine the effects of α-substitution on the spectroscopic, electrochemical, and structural properties of the resulting bis(phthalocyaninato) complexes. We report herein the preparation of three new homoleptic bis[1,8,15,22-tetrakis(3-pentyloxy)phthalocyaninato] rare-earth complexes $[M^{III}\{Pc(\alpha\text{-}OC_5H_{11})_4\}_2]$ (M = Eu, Y, Lu) and a comparison of their properties with those of the non-α-substituted analogues. Due to the four regularly disposed α-substituents (at

[a] R. Wang, R. Li, Y. Bian, P. Zhu, Prof. C. Ma, Prof. J. Jiang
Department of Chemistry, Shandong University
Jinan 250100 (China)
Fax: (+86) 531-856-5211
E-mail: jzjiang@sdu.edu.cn

[b] C.-F. Choi, Prof. D. K. P. Ng
Department of Chemistry
The Chinese University of Hong Kong
Shatin, N.T., Hong Kong (China)
Fax: (+852) 2603-5057
E-mail: dkpn@cuhk.edu.hk

[c] Prof. J. Dou, Prof. D. Wang
Department of Chemistry, Liaocheng University
Liaocheng 252000 (China)

[d] R. D. Hartnell, Dr. D. P. Arnold
Synthesis and Molecular Recognition Program
School of Physical and Chemical Sciences
Queensland University of Technology, G. P. O. Box 2434
Brisbane, Qld. 4001 (Australia)

Supporting information for this article is available on the WWW under http://www.chemeurj.org/ or from the author.

the 1,8,15,22-positions), the two possible cofacial orientations of the phthalocyanine rings give rise to two diastereoisomers with C_{4h} and D_4 molecular symmetry (see Figure 1, assuming that there is a free rotation of the phthalocyaninato ligands about the C_4 axis). The former isomer, which can be partially separated by recrystallization, adopts a slightly distorted square antiprismatic geometry around the metal center, resulting in S_8 symmetry. To the best of our knowledge, this is the first report of rare-earth double-decker complexes with such a molecular symmetry.

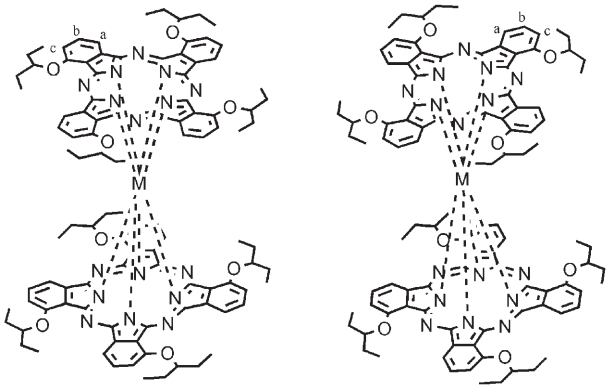

Figure 1. Structures of the two isomers of $[M^{III}\{Pc(\alpha\text{-}OC_5H_{11})_4\}_2]$.

Results and Discussion

Synthesis of $[M^{III}\{Pc(\alpha\text{-}OC_5H_{11})_4\}_2]$: The synthesis involved a simple condensation reaction of the metal-free phthalocyanine $H_2Pc(\alpha\text{-}OC_5H_{11})_4$ with the corresponding metal salts. Thus treatment of $M(acac)_3{\cdot}nH_2O$ (M = Eu, Y, Lu; acac = acetylacetonate) with $H_2Pc(\alpha\text{-}OC_5H_{11})_4$ in refluxing *n*-octanol led to the formation of $[M^{III}\{Pc(\alpha\text{-}OC_5H_{11})_4\}_2]$ [M = Eu (**1**), Y (**2**), Lu (**3**)] via the intermediate $[M^{III}H\{Pc(\alpha\text{-}OC_5H_{11})_4\}_2]$.[8] The yield was higher for the rare earths with a smaller ionic radius (21% for **1**, 45% for **2**, 49% for **3**). This is in line with the trend observed for the other series of bis(phthalocyaninato) complexes $[M^{III}(Pc)_2]$ and $[M^{III}\{Pc(\beta\text{-}OC_8H_{17})_8\}_2]$ (Pc = phthalocyaninate; $Pc(\beta\text{-}OC_8H_{17})_8$ = 2,3,9,10,16,17,23,24-octakis(octyloxy)phthalocyaninate).[8a,9] These three metals were selected because their ionic radii span a relatively wide region, allowing the study of their effects on the spectroscopic and electrochemical properties. The facile characterization of these metal complexes by NMR spectroscopy is also one of the advantages.[10] All the reactions gave a mixture of two isomers with C_{4h} and D_4 symmetry depending on the relative orientation of the two ligands (Figure 1). On the basis of the ^1H NMR data (together with the X-ray diffraction analysis; see below), the former isomer was found to be the major product giving a ratio of 95:5 (for M = Eu) or 7:3 (for M = Y, Lu) with respect to the D_4 isomer. These two isomers could not be separated by column chromatography. However, recrystallization by layering MeOH onto a solution of the mixture in $CHCl_3$ gave some dark-blue cubes, which were found to be the C_{4h} isomer. It seems that this isomer has a higher crystallinity than the D_4 isomer, allowing it to form crystals more readily. Some of the relatively large crystals could be manually separated under a microscope. Thus this method allowed a partial separation of the C_{4h} isomer, but the pure D_4 isomer could not be obtained.

Spectroscopic characterization: The C_{4h} isomers of all the double-deckers were fully characterized with elemental analysis and a wide range of spectroscopic methods (see Table S1 in the Supporting Information). The MALDI-TOF mass spectra showed an isotopic cluster due to the $[M+1]^+$ or $[M+2]^+$ species. The occurrence of the latter signal may be due to the less-negative first reduction potential of these complexes (see below), which allows an ease formation of the monoreduced, protonated $[M^{III}\{Pc(\alpha\text{-}OC_5H_{11})_4\}_2]$ under the experimental conditions. Ionization of this species by protonation leads to the $[M+2]^+$ cluster. A typical spectrum of the C_{4h} isomer of $[Lu^{III}\{Pc(\alpha\text{-}OC_5H_{11})_4\}_2]$ (**3**) is given in Figure S1 (Supporting Information). It can be seen that the isotopic distribution of this cluster is in good agreement with the simulated pattern for the $[M+2]^+$ species.

Like other bis(tetrapyrrole) rare-earth(III) complexes,[10,11] compounds **1**–**3** possess an unpaired electron in one of the macrocyclic ligands, which can be confirmed by EPR spectroscopy. The room-temperature EPR spectra of the Y and Lu analogues in CH_2Cl_2 showed a typical organic radical signal at $g = 2.000$ with a linewidth of 5.1 (for M = Y) or 10.6 G (for M = Lu). As a result of the interaction between the unpaired electron and the paramagnetic Eu^{III} center, the europium counterpart **1** was EPR-silent under these conditions.

^1H NMR spectra of these complexes were recorded in the presence of hydrazine hydrate, which reduced the neutral double-deckers to the corresponding monoanions, thereby making the two macrocyclic ligands become diamagnetic.[12] Figure 2 shows the 2D ^1H–^1H COSY spectrum of the manually separated crystals of the Y analogue **2**. X-ray diffraction analysis revealed that they are the S_8 isomer (see below) or the C_{4h} isomer if we assume that there is a free rotation of the phthalocyaninato ligands about the C_4 axis in solution. All the signals can be readily assigned unambiguously through the correlations established in this experiment. The data together with the assignment are given in Table 1. Interestingly, due to the double-decker structure and the restricted rotation of the 3-pentyloxy substituent, the two ethyl groups of this substituent are no longer equivalent. One of them resonates as two multiplets at $\delta = 2.14$–2.28 and 2.30–2.42 ppm, arising from the two diastereotopic CH_2 protons, and a triplet at $\delta = 1.36$ ppm (CH_3), while the other gives a multiplet at $\delta = 1.98$–2.10 ppm (for the two diastereotopic CH_2 protons) and a triplet at $\delta = 1.12$ ppm (CH_3). The spectrum for the Eu analogue shows similar

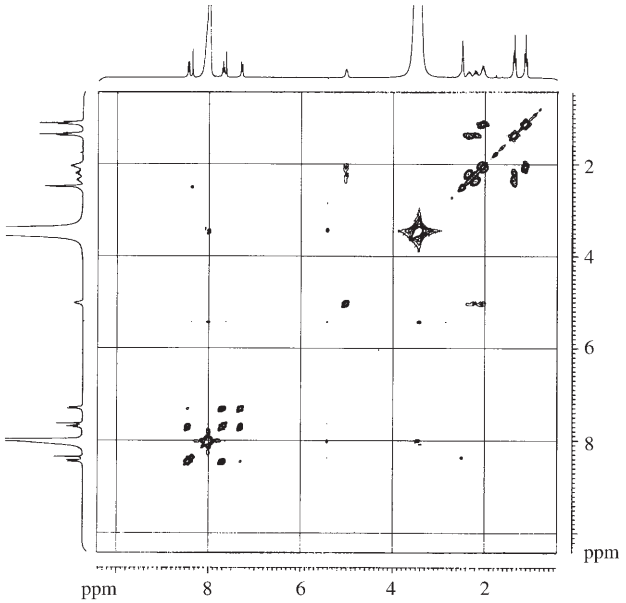

Figure 2. 2D 1H–1H COSY spectrum of the C4h isomer of $[Y^{III}\{Pc(\alpha\text{-}OC_5H_{11})_4\}_2]$ (**2**) in $CDCl_3/[D_6]DMSO$ (1:1) in the presence of approximately 1% hydrazine hydrate.

spectral features, but most of the signals are shifted downfield (Table 1) due to the paramagnetic Eu^{III} center.

^1H NMR data of all the D_4 isomers were obtained from mixtures of the two isomers. These data are also listed in Table 1. In general, two sets of partially overlapped signals for the two isomers were observed. The ratio of the two isomers was determined from the integrations of the two OCH multiplets.

The electronic absorption spectra of the C_{4h} isomers of the three complexes were measured in $CHCl_3$ and the data are compiled in Table 2. The dependence of the spectral features on the metal center is clearly illustrated by the spectra of the Eu, Y, and Lu analogues (Figure 3). The spectra show a typical Soret band at approximately 305 nm with a shoulder at the lower energy side (370–382 nm). The slight splitting of this band has been observed previously for other bis(phthalocyaninato) rare-earth(III) complexes.[8a,12a,13] Interestingly, the Q-bands for these compounds are also split, giving two well-separated absorptions at 628–639 and 707–724 nm as a result of the decrease in molecular symmetry. The spectra for these three compounds also show two weak absorptions at 453–456 and 943–946 nm, which are characteristic π-radical-anion bands for bis(phthalocyaninato) rare-earth(III) complexes.[13,14] These two absorptions have counterparts in the spectra of unsubstituted bis(phthalocyaninato) rare-earth analogues $[M(Pc)_2]$[13,14] and have been assigned to the transitions from the fourth-occupied HOMO to the semi-occupied HOMO and from the semi-occupied HOMO to the LUMO, respectively.[15] However, it is worth noting that the transitions between the phthalocyanine π system and the lone-pair of electrons on the oxygen atoms of the 3-pentyloxy side chains also contribute to the former absorption.[13,14] An additional π-radical-anion marker band appears at 1666–2052 nm, which is significantly red-shifted compared with that of the corresponding $[M^{III}(Pc)_2]$ and $[M^{III}\{Pc(\beta\text{-}OC_nH_{2n+1})_8\}_2]$ ($n=5$, 8),[8a,13b,14] showing that the ring-to-ring interaction is significantly weaker for **1–3**. As shown in Table 2 and Figure 3, all the absorptions (except for the main Soret band at ca. 305 nm) including their position and intensity are sensitive to the metal center.

A simplified molecular orbital diagram of $[M^{III}\{Pc(\alpha\text{-}OC_5H_{11})_4\}_2]$ constructed from the a_{1u} and e_g orbitals of the two ligands is given in Figure 4.[15] The corresponding diagram for $[M^{III}(Pc)_2]$ is also shown for comparison. Due to the more electron-rich $Pc(\alpha\text{-}OC_5H_{11})_4$ with respect to Pc, both the a_{1u} and e_g orbitals of $Pc(\alpha\text{-}OC_5H_{11})_4$ are higher in energy than those of Pc. The weak absorption at 943–946 nm, which shifts slightly to the red with decreasing the size of the metal center, is due to the electronic transition from the semi-occupied orbital to the degenerate LUMO. The lowest energy near-IR band at 1666–2052 nm is due to the transition from the second-highest occupied orbital to

Table 1. ^1H NMR data [δ in ppm] for the reduced form of $[M^{III}\{Pc(\alpha\text{-}OC_5H_{11})_4\}_2]$ (M = Eu (**1**), Y (**2**), Lu (**3**)).

	H_a	H_b	H_c	OCH	CH_2	CH_3
1 C_{4h}[a]	10.11 (d, J = 7.5 Hz, 8H)	8.32 (t, J = 7.5 Hz, 8H)	7.90 (d, J = 7.5 Hz, 8H)	6.48–6.58 (m, 8H)	2.84–2.96 (m, 16H)[c]	1.57 (t, J = 7.5 Hz, 24H)[c]
1 D_4[b]	10.28 (d, J = 7.3 Hz, 8H)	8.40 (t, J = 7.3 Hz, 8H)	–[c]	6.07 (m, 8H)	3.11 (m)[c]	1.16 (t, J = 7.3 Hz, 24H)[c]
2 C_{4h}[a]	8.44 (d, J = 7.5 Hz, 8H)	7.70 (t, J = 7.5 Hz, 8H)	7.30 (d, J = 7.5 Hz, 8H)	5.00–5.06 (m, 8H)	2.30–2.42 (m, 8H)	1.36 (t, J = 7.5 Hz, 24H)
					2.14–2.28 (m, 8H)	1.12 (t, J = 7.5 Hz, 24H)
					1.98–2.10 (m, 16H)	
2 D_4[b]	8.47 (d, J = 7.3 Hz, 8H)	7.74 (t, J = 7.3 Hz, 8H)	7.28 (d, J = 7.3 Hz, 8H)	4.81 (m, 8H)	2.20 (m)	1.37 (t, J = 7.3 Hz, 24H)
					2.05 (m)	0.90 (t, J = 7.3 Hz, 24H)
					1.85 (m)	
3 C_{4h}[b]	8.45 (d, J = 7.3 Hz, 8H)	7.70 (t, J = 7.3 Hz, 8H)	7.30 (d, J = 7.3 Hz, 8H)	4.98–5.04 (m, 8H)	2.32–2.44 (m, 8H)	1.11 (t, J = 7.4 Hz, 24H)
					2.25–2.30 (m, 8H)	1.37 (t, J = 7.4 Hz, 24H)
					2.00–2.10 (m, 16H)	
3 D_4[b]	8.47 (d, J = 7.3 Hz, 8H)	7.74 (t, J = 7.3 Hz, 8H)	7.28 (d, J = 7.3 Hz, 8H)	4.81 (m)	2.20 (m)	1.39 (t, J = 7.3 Hz, 24H)
					2.05 (m)	0.89 (t, J = 7.3 Hz, 24H)
					1.85 (m)	

[a] Recorded in $CDCl_3/[D_6]DMSO$ (1:1) with the addition of ca. 1% (by volume) hydrazine hydrate on a 300 MHz spectrometer unless otherwise stated. [b] Recorded in $CDCl_3/[D_6]DMSO$ (1:1) with the addition of ca. 10% (by volume) hydrazine hydrate on a 400 MHz spectrometer. The data were taken from the spectra of mixtures containing both isomers. [c] These signals were not observed due to an overlap with the strong bands of water, hydrazine, or residual solvents.

Table 2. Electronic absorption data for $[M^{III}\{Pc(\alpha\text{-}OC_5H_{11})_4\}_2]$ (M = Eu (**1**), Y (**2**), Lu (**3**)) in $CHCl_3$.

	λ_{max} [nm] ($\log\varepsilon$)						
C_{4h} isomer of **1**	305 (4.98)	382 (sh)	453 (sh)	639 (5.03)	724 (5.00)	943 (3.40)	2052 (4.17)
C_{4h} isomer of **2**	306 (5.00)	377 (sh)	454 (sh)	632 (4.99)	713 (5.11)	945 (3.57)	1816 (4.20)
C_{4h} isomer of **3**	305 (5.02)	370 (sh)	456 (sh)	628 (4.96)	707 (5.19)	946 (3.72)	1666 (4.21)

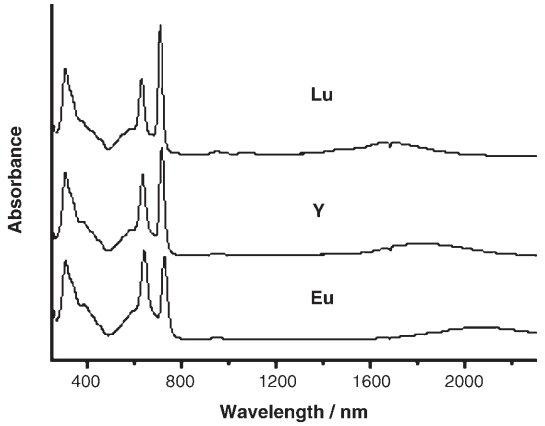

Figure 3. Electronic absorption spectra of the C_{4h} isomers of $[M^{III}\{Pc(\alpha\text{-}OC_5H_{11})_4\}_2]$ (M = Eu, Y, Lu) (**1**–**3**) in $CHCl_3$.

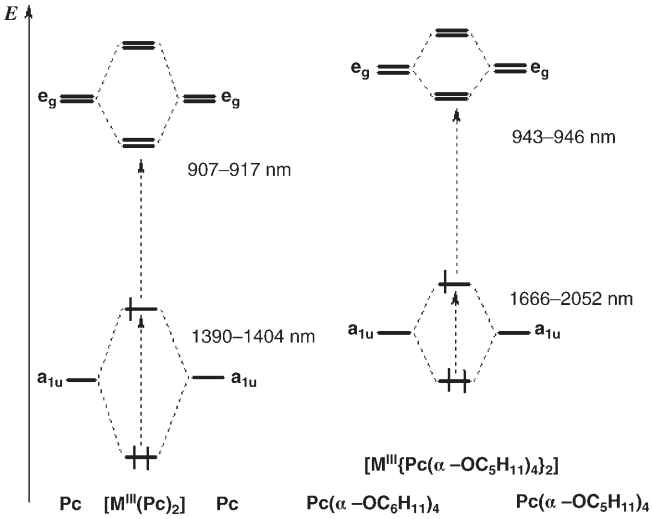

Figure 4. Simplified molecular orbital diagrams for $[M^{III}(Pc)_2]$ and $[M^{III}\{Pc(\alpha\text{-}OC_5H_{11})_4\}_2]$.

the semi-occupied orbital.[16] The energy involved, which reflects the extent of electronic coupling between the two macrocycles, increases from compound **1**–**3**. This suggests that as the size of the metal center decreases, there is a stronger π–π interaction in the complex.

The presence of an unpaired electron in one of the phthalocyaninato ligands was supported by vibrational spectroscopy. An intense band at 1307–1315 cm^{-1} together with a medium band at approximately 1380 cm^{-1} were observed in the IR spectra of the C_{4h} isomers of **1**–**3**. These are the characteristic bands for phthalocyanine radical anion and dianion, respectively.[17] With laser excitation at 632.8 nm, the marker Raman band for the $[Pc(\alpha\text{-}OC_5H_{11})_4]^{\bullet-}$ radical anion appeared in the range of 1522–1530 cm^{-1} for the C_{4h} isomers of **1**–**3**.[18]

Structural studies: Single crystals of the C_{4h} isomer of $[Y^{III}\{Pc(\alpha\text{-}OC_5H_{11})_4\}_2]$ (**2**) suitable for X-ray diffraction analysis were obtained by slow diffusion of MeOH into a solution of the sample in $CHCl_3$. This compound represents the first example of a homoleptic bis(1,8,15,22-tetrasubstituted phthalocyaninato)metal complex that has been structurally characterized. The compound crystallizes in the monoclinic system with four molecules per unit cell. Figure 5 shows a

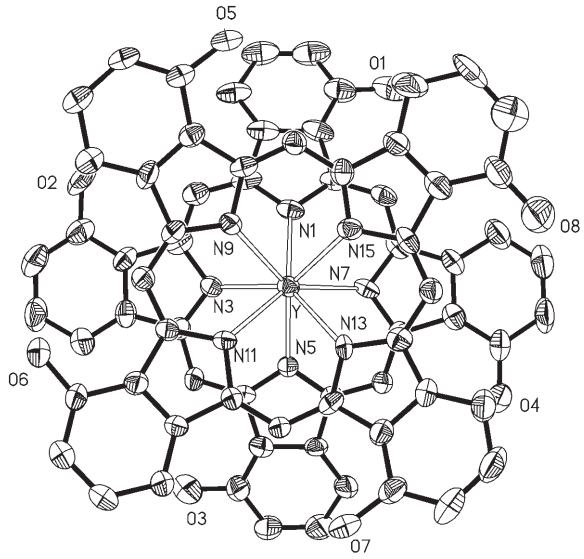

Figure 5. Molecular structure of the C_{4h} isomer of $[Y^{III}\{Pc(\alpha\text{-}OC_5H_{11})_4\}_2]$ (**2**) showing the 30% probability thermal ellipsoids for all non-hydrogen atoms.

perspective view of the structure. The yttrium center is eight-coordinate, bound to the isoindole nitrogen atoms of the two tetra-α-substituted phthalocyaninato ligands. The two ligands are almost fully staggered forming a slightly distorted square antiprism. Thus the compound exhibits a pinwheel-like S_8 symmetry in the solid state, which has not been observed previously for this class of compounds. The yttrium atom lies almost in the center between the two Pc-$(\alpha\text{-}OC_5H_{11})_4$ rings (1.350 vs 1.368 Å). Like the structures of many tetrapyrrole double-decker complexes,[11] the two ligands are not planar and display a saucer shape.

Electrochemical properties: The redox behavior of the C_{4h} isomers of **1**–**3** was studied by cyclic voltammetry (CV) and differential pulse voltammetry (DPV) in CH_2Cl_2. All the

three compounds showed three quasi-reversible one-electron oxidations and three quasi-reversible one-electron reductions, which can be attributed to the successive removal of electrons from and addition of electrons to the ligand-based orbitals, respectively, as the trivalent rare-earth metal center cannot be oxidized or reduced under these conditions. Figure 6 shows the voltammograms for the yttrium an-

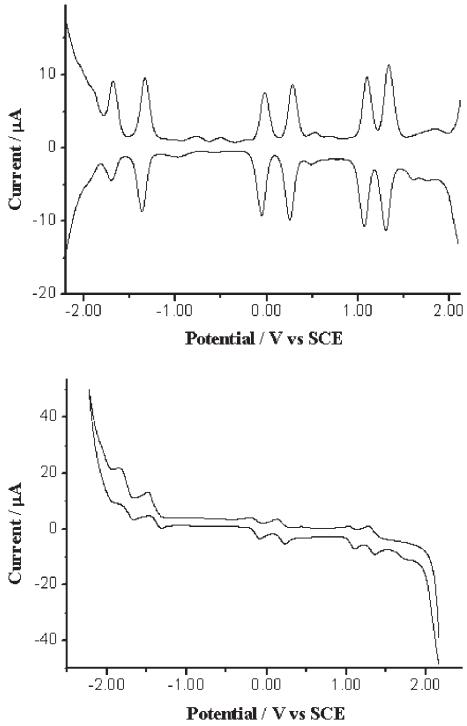

Figure 6. Cyclic voltammogram (bottom) and differential pulse voltammogram (top) of the C_{4h} isomer of $[Y^{III}\{Pc(\alpha\text{-}OC_5H_{11})_4\}_2]$ (**2**) in CH_2L_2 containing 0.1 mol dm^{-3} $[NBu_4][ClO_4]$ at a scan rate of 20 and 10 mV s^{-1}, respectively.

alogue, which are very similar to those for the other two double-deckers. The data are collected in Table 3. The electrochemical data for **1–3**, as a mixture of the C_{4h} and D_4 isomers, were also measured. The data were virtually identical ($\pm$0.03 V at most) with those obtained from the corresponding pure C_{4h} isomer.

Compared with the electrochemical data of the corresponding $[M^{III}(Pc)_2]$,[19] the oxidation potentials of $[M^{III}\{Pc(\alpha\text{-}OC_5H_{11})_4\}_2]$ (**1–3**) are lower by 0.23–0.54 V and their reduction potentials are more negative by 0.18–0.44 V, reflecting the electron-donating nature of the 3-pentyloxy group. The gap between Oxd_2 and Oxd_1 ($\Delta E'_{1/2}$) reflects the energy separation between the semi-occupied orbital and the second-highest occupied orbital. The value is significantly smaller for $[M^{III}\{Pc(\alpha\text{-}OC_5H_{11})_4\}_2]$ (0.82–0.95 vs 1.04–1.20 V for $[M^{III}(Pc)_2]$). This also shows that the π–π interaction is weaker for these bis(tetra-α-substituted phthalocyaninato) rare-earth complexes. In contrast, the potential difference between Red_1 and Red_2 ($\Delta E''_{1/2}$), which represents the gap between the semi-occupied orbital and the LUMO, is only marginally larger for$[M^{III}\{Pc(\alpha\text{-}OC_5H_{11})_4\}_2]$ (1.20–1.29 vs. 1.08–1.19 V for $[M^{III}(Pc)_2]$). This is in accord with the results for the double-deckers $[M^{III}\{Pc(\beta\text{-}tBu)_4\}_2]$ and $[M^{III}\{Pc(\beta\text{-}OC_8H_{17})_8\}_2]$.[19] For these complexes, the introduction of the electron-donating *tert*-butyl and octyloxy groups also induces a cathodic shift of all redox processes without significantly changing the relative energy levels of the semi-occupied orbital and the LUMO.

Furthermore, the difference of the redox potentials of Red_1 and Red_2 for $[M^{III}\{Pc(\alpha\text{-}OC_5H_{11})_4\}_2]$ actually corresponds to the potential difference between the first oxidation and first reduction processes of $[M^{III}\{Pc(\alpha\text{-}OC_5H_{11})_4\}_2]^-$, which gradually decreases from 1.29 to 1.20 mV along with the decrease of rare-earth radius. As the first oxidation step and first reduction step, involve the HOMO and the LUMO of the molecule, respectively, the energy difference between these two redox processes for $[M^{III}\{Pc(\alpha\text{-}OC_5H_{11})_4\}_2]^-$ corresponds to its electrochemical molecular band gap. The value $\Delta E''_{1/2}$ thus should reflect the energy necessary for the transition of an electron from the HOMO to the LUMO of $[M^{III}\{Pc(\alpha\text{-}OC_5H_{11})_4\}_2]^-$ and therefore should correlate with the lowest energy optical transition in the electronic absorption spectrum of $[M^{III}\{Pc(\alpha\text{-}OC_5H_{11})_4\}_2]^-$. In fact, the decreasing trend observed for the $\Delta E''_{1/2}$ value of these bis(phthalocyaninato) rare-earth complexes along with the lanthanide contraction is in good agreement with the red-shift of the lowest electronic absorption band of $[M^{III}\{Pc(\alpha\text{-}OC_5H_{11})_4\}_2]^-$, from 692 nm for M = Eu to 701 nm for M = Lu, along with the same order (Figure S2 in the Supporting Information).

As shown in Table 3, the potentials of both Oxd_1 and Red_1 are slightly shifted to the cathodic side along with the decrease in metal size (i.e., from **1** to **3**). These potentials are related to the energy level of the semi-occupied molecular orbital. In contrast, the potentials of both Oxd_2 and Oxd_3, which involve the second-highest occupied orbital, remain more or less the same. These results reveal that along with lanthanide contraction, the energy gap between the semi-occupied molecular orbital and the second-highest occupied orbital increases, showing an increase in π–π interaction as the size of the metal center decreases. This is in line with the

Table 3. Electrochemical data for the C_{4h} isomers of **1–3**.[a]

	Oxd_3	Oxd_2	Oxd_1	Red_1	Red_2	Red_3	$\Delta E_{1/2}$[b]	$\Delta E'_{1/2}$[c]	$\Delta E''_{1/2}$[d]
C_{4h} isomer of **1**	+1.29	+1.05	+0.23	−0.09	−1.38	−1.73	0.32	0.82	1.29
C_{4h} isomer of **2**	+1.32	+1.07	+0.18	−0.14	−1.38	−1.74	0.32	0.89	1.24
C_{4h} isomer of **3**	+1.32	+1.07	+0.12	−0.20	−1.40	−1.75	0.32	0.95	1.20

[a] Recorded with $[Bu_4N][ClO_4]$ as electrolyte in CH_2Cl_2 (0.1 mol dm^{-3}) at ambient temperature. Potentials were obtained by cyclic voltammetry with a scan rate of 20 mV s^{-1}, and are expressed as half-wave potentials ($E_{1/2}$) in V relative to SCE unless otherwise stated. [b] $\Delta E_{1/2} = Oxd_1 - Red_1$. [c] $\Delta E'_{1/2} = Oxd_2 - Oxd_1$. [d] $\Delta E''_{1/2} = Red_1 - Red_2$.

hypsochromic shift of the longest wavelength near-IR band described above. The remaining reduction processes Red_2 and Red_3 are not sensitive to the rare-earth metal center. This indicates that the energy level of the LUMO (as well as the remaining unoccupied orbitals) remains relatively unchanged along the series.

The values of $\Delta E_{1/2}$, that is, the potential difference between Oxd_1 and Red_1, are identical for **1**–**3**. The value (0.32 V) is significantly smaller than the corresponding values for $[M(Pc')_2]$ ($Pc' = Pc$, $Pc(\beta\text{-}t\text{Bu})_4$, $Pc(\beta\text{-}OC_8H_{17})_8$: 0.41–0.45 V).[19]

Conclusion

In summary, we have prepared three novel homoleptic bis(1,8,15,22-tetrasubstituted phthalocyaninato) rare-earth complexes $[M^{III}\{Pc(\alpha\text{-}OC_5H_{11})_4\}_2]$ ($M = Eu$, Y, Lu). The C_{4h} isomers of these compounds can be partially separated by recrystallization and it has been confirmed by X-ray diffraction analysis that they adopt an usual pinwheel-like structure with S_8 symmetry in the solid state. Spectroscopic and electrochemical studies have revealed that these complexes have a weaker π–π interaction compared with the unsubstituted or β-substituted bis(phthalocyaninato) analogues.

Experimental Section

Purification of solvents, preparation of precursors, spectroscopic measurements, and electrochemical studies have been described in detail elsewhere.[6b]

General procedure for the preparation of 1–3: In a typical procedure, a mixture of $M(acac)_3{\cdot}nH_2O$ ($M = Eu$, Y, Lu) (30 mg, 0.06 mmol) and $H_2Pc(\alpha\text{-}OC_5H_{11})_4$ (85 mg, 0.10 mmol) in *n*-octanol (4 mL) was heated at 200 °C under nitrogen for 9 h. The mixture was cooled to room temperature, then the volatiles were evaporated under reduced pressure, and the residue was subjected to chromatography on a silica-gel column using $CHCl_3$ as eluent. Following the green fraction containing a small amount of unreacted $H_2Pc(\alpha\text{-}OC_5H_{11})_4$, a blue band with the target homoleptic double-decker $[M\{Pc(\alpha\text{-}OC_5H_{11})_4\}_2]$ was developed, which was followed by another green band containing the protonated, reduced double-decker $[MH\{Pc(\alpha\text{-}OC_5H_{11})_4\}_2]$. The crude product was purified by repeated chromatography followed by recrystallization from $CHCl_3$/MeOH. Some relatively large dark-blue crystals of the C_{4h} isomer could be separated under a microscope. Yield: 21 % for **1**, 45 % for **2**, 49 % for **3**.

X-ray crystallographic analysis of the C_{4h} isomer of 2: Crystal data and details of data collection and structure refinement are given in Table 4. Data were collected on a Bruker SMART CCD diffractometer with an $Mo_{K\alpha}$ sealed tube ($\lambda = 0.71073$ Å) at 293 K, and by using a ω scan mode with an increment of 0.3°. Preliminary unit cell parameters were obtained from 45 frames. Final unit cell parameters were derived by global refinements of reflections obtained from integration of all the frame data. The collected frames were integrated by using the preliminary cell-orientation matrix. SMART software was used for collecting frames of data, indexing reflections, and determination of lattice constants; SAINT-PLUS for integration of intensity of reflections and scaling;[20] SADABS for absorption correction;[21] and SHELXL for space group and structure determination, refinements, graphics, and structure reporting.[22] CCDC-256203 contains the supplementary crystallographic data for this paper. These data can be obtained free of charge from The Cambridge Crystallographic Data Centre via www.ccdc.cam.ac.uk/data_request/cif.

Table 4. Crystallographic data for the C_{4h} isomer of **2**.

	C_{4h} isomer of **2**
formula	$C_{104}H_{112}N_{16}O_8Y$
M_r	1803.0
crystal size [mm^3]	$0.52 \times 0.43 \times 0.04$
crystal system	monoclinic
space group	$P2_1/n$
a [Å]	19.535(3)
b [Å]	14.855(2)
c [Å]	32.658(5)
β [°]	93.781(3)
V [Å^3]	9457(2)
Z	4
$F(000)$	3804
ρ_{calcd} [Mg m^{-3}]	1.266
μ [mm^{-1}]	0.683
θ range [°]	1.72 to 24.00
reflections collected	44148
independent reflections	14774 ($R_{int} = 0.1565$)
parameters	1166
$R1$ [$I > 2\sigma(I)$]	0.0860
w$R2$ [$I > 2\sigma(I)$]	0.1870
goodness of fit	0.965

Acknowledgements

We thank Profs. Yunqi Liu and Hung-Kay Lee for recording the EPR spectra, and Dr. L. Rintoul for recording the Raman spectra. Financial support from the National Science Foundation of China (Grant No. 20325105, 20431010), National Ministry of Science and Technology of China (Grant No. 2001CB6105–7), National Ministry of Education of China, Shandong University, The Chinese University of Hong Kong, and the Science Research Centre of Queensland University of Technology is gratefully acknowledged.

[1] a) J. Souto, R. Aroca, J. A. DeSaja, *J. Phys. Chem.* **1994**, *98*, 8998–9001; b) K. R. Rickwood, D. R. Lovett, B. Lukas, J. Silver, *J. Mater. Chem.* **1995**, *5*, 725–729; c) P. Bassoul, T. Toupance, J. Simon, *Sens. Actuators B* **1995**, *26/27*, 150–152; d) M. L. Rodríguez-Méndez, Y. Gorbunova, J. A. de Saja, *Langmuir* **2002**, *18*, 9560–9565; e) T. Komatsu, K. Ohta, T. Fujimoto, I. Yamamoto, *J. Mater. Chem.* **1994**, *4*, 533–536; f) R. Jones, A. Krier, K. Davidson, *Thin Solid Films* **1997**, *298*, 228–236.

[2] a) K. Yoshino, S. B. Lee, T. Sonoda, H. Kawagishi, R. Hidayat, K. Nakayama, M. Ozaki, K. Ban, K. Nishizawa, K. Ohta, H. Shirai, *J. Appl. Phys.* **2000**, *88*, 7137–7143; b) L. Galmiche, F. Guyon, A. Pondaven, J.-Y. Moisan, M. L'Her, *J. Porphyrins Phthalocyanines* **2003**, *7*, 382–387; c) L. Cao, H.-Z. Chen, H.-B. Zhou, L. Zhu, J.-Z. Sun, X.-B. Zhang, J.-M. Xu, M. Wang, *Adv. Mater.* **2003**, *15*, 909–913.

[3] a) M. Guéna, Z. Y. Wu, M. L'Her, A. Pondaven, C. Cadiou, *Appl. Phys. Lett.* **1998**, *72*, 765–767; b) G. A. Kumar, *J. Nonlinear Opt. Phys. Mater.* **2003**, *12*, 367–376.

[4] a) N. Ishikawa, M. Sugita, T. Ishikawa, S. Koshihara, Y. Kaizu, *J. Am. Chem. Soc.* **2003**, *125*, 8694–8695; b) N. Ishikawa, M. Sugita, T. Ishikawa, S. Koshihara, Y. Kaizu, *J. Phys. Chem. B* **2004**, *108*, 11265–11271; c) N. Ishikawa, M. Sugita, T. Okubo, N. Tanaka, T. Lino, SY. Kaizu, *Inorg. Chem.* **2003**, *42*, 2440–2446; d) N. Ishikawa, M. Sugita, W. Wernsdorfer, *J. Am. Chem. Soc.* **2005**, *127*, 3650–3651.

[5] R. Weiss, J. Fischer, in *The Porphyrin Handbook, Vol. 16* (Eds.: K. M. Kadish, K. M. Smith, R. Guilard), Academic Press, San Diego, **2003**, pp. 171–246.

[6] a) Y. Bian, R. Wang, J. Jiang, C.-H. Lee, J. Wang, D. K. P. Ng, *Chem. Commun.* **2003**, 1194–1195; b) Y. Bian, R. Wang, D. Wang, P. Zhu, R. Li, J. Dou, W. Liu, C.-F. Choi, H.-S. Chan, C. Ma, D. K. P. Ng, J.

Jiang, *Helv. Chim. Acta* **2004**, *87*, 2581–2596; c) R. Wang, Y. Li, R. Li, D. Y. Y. Cheng, P. Zhu, D. K. P. Ng, M. Bao, X. Cui, N. Kobayashi, J. Jiang, *Inorg. Chem.* **2005**, *44*, 2114–2120.

[7] N. Kobayashi, H. Ogata, N. Nonaka, E. A. Luk'yanets, *Chem. Eur. J.* **2003**, *9*, 5123–5134.

[8] a) W. Liu, J. Jiang, D. Du, D. P. Arnold, *Aust. J. Chem.* **2000**, *53*, 131–135; b) J. Jiang, W. Liu, K.-W. Poon, D. Du, D. P. Arnold, D. K. P. Ng, *Eur. J. Inorg. Chem.* **2000**, 205–209.

[9] C. Clarisse, M. T. Riou, *Inorg. Chim. Acta* **1987**, *130*, 139–144.

[10] J. Jiang, Y. Bian, F. Furuya, W. Liu, M. T. M. Choi, H. W. Li, N. Kobayashi, Q. Yang, T. C. W. Mak, D. K. P. Ng, *Chem. Eur. J.* **2001**, *7*, 5059–5069.

[11] a) D. K. P. Ng, J. Jiang, *Chem. Soc. Rev.* **1997**, *26*, 433–442; b) J. W. Buchler, D. K. P. Ng in *The Porphyrin Handbook, Vol. 3* (Eds.: K. M. Kadish, K. M. Smith, R. Guilard), Academic Press, San Diego, **2000**, pp. 245–294; c) J. Jiang, K. Kasuga, D. P. Arnold in *Supramolecular Photosensitive and Electroactive Materials* (Ed.: H. S. Nalwa), Academic Press, New York, **2001**, pp. 113–210.

[12] a) A. Pondaven, Y. Cozien, M. L'Her, *New J. Chem.* **1992**, *16*, 711–718; b) F. Guyon, A. Pondaven, P. Guenot, M. L'Her, *Inorg. Chem.* **1994**, *33*, 4787–4793.

[13] a) J. Jiang, W. Liu, W.-F. Law, J. Lin, D. K. P. Ng, *Inorg. Chim. Acta* **1998**, *268*, 141–144; b) J. Jiang, J. Xie, M. T. M. Choi, Y. Yan, S. Sun, D. K. P. Ng, *J. Porphyrins Phthalocyanines* **1999**, *3*, 322–328.

[14] a) J. Jiang, R. C. W. Liu, T. C. W. Mak, T. W. D. Chan, D. K. P. Ng, *Polyhedron* **1997**, *16*, 515–520; b) D. Markovitsi, T.-H. Tran-Thi, R. Even, J. Simon, *Chem. Phys. Lett.* **1987**, *137*, 107–112; c) W.-F. Law, R. C. W. Liu, J. Jiang, D. K. P. Ng, *Inorg. Chim. Acta* **1997**, *256*, 147.

[15] a) E. Orti, J. L. Bredas, C. Clarisse, *J. Chem. Phys.* **1990**, *92*, 1228–1235; b) R. Rousseau, R. Aroca, M. L. Rodriguez-Mendez, *J. Mol. Struct.* **1995**, *356*, 49–62; c) N. Ishikawa, *J. Porphyrins Phthalocyanines* **2001**, *5*, 87–101.

[16] According to the "supermolecular" MO model, this characteristic absorption can be attributed to the electronic transition from the second-highest-filled supermolecular bonding orbital to the half-filled supermolecular antibonding orbital. See a) J. K. Duchowski, D. F. Bocian, *J. Am. Chem. Soc.* **1990**, *112*, 3312–3318; b) O. Bilsel, J. Rodriguez, S. N. Milam, P. A. Gorlin, G. S. Girolami, K. S. Suslick, D. Holten, *J. Am. Chem. Soc.* **1992**, *114*, 6528–6538.

[17] a) J. Jiang, D. P. Arnold, H. Yu, *Polyhedron* **1999**, *18*, 2129–2139; b) F. Lu, M. Bao, C. Ma, X. Zhang, D. P. Arnold, J. Jiang, *Spectrochim. Acta A* **2003**, *59*, 3273–3286.

[18] a) J. Jiang, L. Rintoul, D. P. Arnold, *Polyhedron* **2000**, *19*, 1381–394; b) J. Jiang, U. Cornelissen, D. P. Arnold, X. Sun, H. Homborg, *Polyhedron* **2001**, *20*, 557–569.

[19] P. Zhu, F. Lu, N. Pan, D. P. Arnold, S. Zhang, J. Jiang, *Eur. J. Inorg. Chem.* **2004**, 510–517.

[20] SMART and SAINT for Windows NT Software Reference Manuals, Version 5.0, Bruker Analytical X-Ray Systems, Madison, Wisconsin, **1997**.

[21] G. M. Sheldrick, SADABS, A Software for Empirical Absorption Correction, University of Göttingen, Germany, **1997**.

[22] SHELXL Reference Manual, Version 5.1, Bruker Analytical X-Ray Systems, Madison, Wisconsin, **1997**.

Received: February 25, 2005
Published online: September 15, 2005

